Jurnal Ilmiah Teknik Elektro Komputer dan Informatika (JITEKI)
Vol. 10, No. 4, December 2024, pp. 704-722
ISSN: 2338-3070, DOI: 10.26555/jiteki.v10i4.30221

Techno-Economic Optimization and Sensitivity Analysis of a Hybrid Grid-Connected Microgrid System for Sustainable Energy

Habib Muhammad Usman[1], Nirma Kumari Sharma[1], Deepak Kumar Joshi[1], Aditya Kaushik[1], Suraj Kumhar[1], Sani Saminu[2], Abdulbasid Bashir Yero[3]
[1]Department of Electrical Engineering, Mewar University, Chittorgarh, Rajathan, India
[2]Department of Biomedical Engineering, University of Ilorin, Ilorin, Nigeria
[3]Department of Electrical and Electronics Engineering, Nile University of Nigeria

ARTICLE INFO

Article history:

Received October 07, 2024
Revised December 04, 2024
Published December 08, 2024

Keywords:

Renewable energy sources (RES);
Levelized cost of energy (LCOE);
HOMER software;
Economical analysis;
Sensitivity analysis;
Optimization;
Microgrid

ABSTRACT

Chittorgarh like many other villages in India faces a dual challenge of unreliable electricity supply and heavy dependence on fossil fuels, which undermines economic development and environmental sustainability. Addressing this critical issue, this study explores the optimization of a hybrid grid-connected microgrid comprising wind turbines, solar photovoltaic (PV) systems, and grid integration, aimed at delivering reliable, sustainable, and cost-effective energy. To achieve this, real-world meteorological and energy pricing data were analyzed, and HOMER software was employed for comprehensive system modeling. The proposed microgrid features a 165,024 kW wind turbine system and a 1,500 kW solar PV system, generating a combined annual energy production of 58,772,300 kWh. Wind energy dominates the energy mix, contributing 35,272,200 kWh/year, with a capacity factor of 29%, while solar PV provides 23,500,100 kWh/year with a capacity factor of 22%. Both systems efficiently operate for 4,327 hours/year, supplying a primary AC load of 20,077,351 kWh/year, thereby ensuring reliable energy delivery. Economic analysis reveals that the system's total capital investment is $8.6 million, with replacement and operations and maintenance (O&M) costs amounting to $4.5 million and $3.5 million, respectively. The system demonstrates exceptional economic viability, achieving a Levelized Cost of Energy (LCOE) of $0.0413/kWh, a present worth of $16.6 million, and an annual worth of $1.99 million, delivering a 12% return on investment (ROI). Additionally, the microgrid operates as a net energy exporter, selling 46,979,478 kWh/year to the grid and generating a net annual profit of $53,748, with peak profitability recorded in May ($53,553) and June ($47,615). Sensitivity analysis was conducted under various scenarios, including variations in solar irradiance, wind speed, fuel prices, energy production, and grid prices, to evaluate the robustness of the system's performance and economic metrics. The analysis highlights the resilience of the microgrid design, showcasing its adaptability to diverse operational conditions while maintaining economic and environmental viability. The findings provide compelling evidence for policymakers, investors, and energy stakeholders to adopt renewable energy systems that combine sustainability, reliability, and profitability. By leveraging these insights, similar energy-deficient regions can achieve significant strides toward energy independence and environmental preservation.

Corresponding Author:

Habib Muhammad Usman, Department of Electrical Engineering, Mewar University, chittorgarh, Rajathan, India
Email: Habibusman015@gmail.com

1. INTRODUCTION

Global energy consumption is projected to rise by 50% by 2050, primarily due to population growth and economic development. Fossil fuels currently dominate the global energy mix, comprising over 81% of the world's energy consumption, as reported by the International Energy Agency (IEA) [1]. This dependence on fossil fuels drives global greenhouse gas emissions, releasing approximately 34 billion tons of CO2 annually, with coal, oil, and natural gas contributing 45%, 35%, and 20% of these emissions, respectively. Such reliance has intensified environmental issues, including escalating greenhouse gas emissions, climate change, and widespread air pollution [2]–[4]. The environmental consequences are profound, with rising global temperatures, increased frequency of extreme weather events, and accelerating sea-level rise directly linked to heightened greenhouse gas concentrations. These changes pose significant threats to ecosystems, human health, and global economies. Furthermore, the volatility of fossil fuel markets, exacerbated by geopolitical tensions and fluctuating oil prices, highlights the instability and insecurity associated with these energy sources [5]–[7].

In light of these challenges, a transition to sustainable energy solutions is increasingly urgent. Renewable energy sources, such as solar, wind, and hydropower, offer compelling advantages [8]. They are environmentally benign, economically feasible, and provide sustainable alternatives to traditional fossil fuels. Their widespread availability and local accessibility bolster energy security by diversifying energy portfolios and reducing reliance on imported fuels. Transitioning to renewables is pivotal for mitigating the adverse environmental impacts of fossil fuels and establishing a resilient and sustainable energy landscape [9]–[11]. Addressing climate change and ensuring a reliable energy supply for future generations necessitates a comprehensive transition to renewable energy sources. This transition not only mitigates environmental challenges but also delivers economic benefits and enhances energy security. Investments in sustainable energy solutions can significantly reduce greenhouse gas emissions, stabilize energy markets, and promote a healthier planet. By integrating diverse renewable energy sources such as solar and wind, we can harness their complementary strengths to address intermittency issues and optimize energy production. This synergy improves grid stability, reduces dependence on fossil fuels, and substantially contributes to carbon emission reductions and environmental conservation [12], [13]. Furthermore, adopting a hybrid renewable energy approach fosters innovation in energy storage technologies and grid management systems, paving the way for a more resilient and sustainable energy landscape worldwide [14]–[16]. Hybrid renewable energy systems (HRES) blend renewable sources like solar, wind, and biomass with conventional energy systems or storage solutions, ensuring consistent and reliable electricity supply by managing generation and demand fluctuations effectively (Table 1). For instance, combining solar panels with wind turbines or integrating battery storage optimizes energy utilization, enhances grid stability, and reduces energy costs. This approach addresses energy security challenges while accelerating the shift toward cleaner energy, supporting both environmental preservation and economic growth [17], [18].

Recent studies have explored the potential of HRES in various contexts. Alshammari *et al.* [22] investigated a standalone system incorporating wind, biomass, photovoltaics, and battery storage for island energy generation, identifying an optimal configuration with a COE of $0.254/kWh. However, their focus on standalone systems excludes the advantages of grid-connected systems in urban settings, where battery storage may not be necessary. Similarly, Kharrich *et al.* [23] analyzed a hybrid microgrid powered by renewable energy using optimization algorithms like Multi-Objective Particle Swarm Optimization (MOPSO) and Strength Pareto Evolutionary Algorithm 2 (SPEA2). While their findings demonstrated the effectiveness of SPEA2 in reducing NPC and CO2 emissions, the study's focus on remote microgrids limits its applicability to urban areas where grid connectivity and spatial constraints are critical considerations. Usman *et al.* [24] designed microgrid with biomass as a fuel for generating electricity.

Conteh *et al.* [25] examined sustainable electrification in Lungi Town, Sierra Leone, utilizing a genetic algorithm to evaluate hybrid renewable energy system (HRES) configurations. They identified a cost-effective wind/PV/diesel generator/battery setup; however, the reliance on diesel and battery storage raises concerns about feasibility in urban university campuses, where grid-connected renewable energy systems may offer greater economic and environmental advantages. Moreover [26] proposed a design modification and performance evaluation of a solar PV system tailored for an AutoCAD laboratory. Their study focused on optimizing the PV system configuration to meet the specific energy demands of the laboratory, emphasizing enhanced energy output and cost-effectiveness. Ma *et al.* [27] conducted a feasibility and techno-economic assessment of a standalone solar-wind hybrid system with battery storage for a remote island, using 2009 solar and wind data. Using HOMER software, they optimized the system based on net present cost (NPC) and cost of electricity (COE), achieving a COE of $0.595/kWh. While their findings highlight reliability and economic sensitivity to component capacities, they do not address urban challenges such as space constraints, higher energy demands, and the absence of battery storage, which are critical for grid-connected systems. Authors in

[28] proposed the implementation of wind-powered agriculture to enhance crop production and economic prosperity in arid regions. Their study highlighted the use of wind energy to power irrigation systems, ensuring a reliable water supply for agricultural activities in areas with limited access to conventional energy sources. The research demonstrated that integrating wind power not only improves crop yields but also reduces operational costs, contributing to the economic sustainability of farming in these challenging environments.

Nandi *et al.* [29] proposed a wind-PV-battery hybrid system for community loads, leveraging wind data from 2006 and solar data from 1992–2003. With a COE of $0.363/kWh and a 25-ton annual CO2 reduction, the study demonstrated feasibility for off-grid communities. However, the use of outdated data limits applicability to current technologies, and the rural focus leaves a gap in understanding urban applications. Al-Sharafi *et al.* [30] assessed solar and wind potentials across Saudi Arabia, identifying a cost-effective off-grid system in Yanbu with a COE of $0.609/kWh. Despite valuable regional insights, their analysis does not explore grid-connected systems that omit battery storage, particularly relevant in urban settings where cost and space efficiency are priorities.

Nouadje *et al.* [31] analyzed a hybrid energy system in Woulde, Cameroon, integrating geothermal, biogas, wind, and PV technologies with Demand-Actuated Technology (DAT). Their findings revealed that DAT reduced battery requirements and energy costs, lowering COE from $0.271/kWh to $0.260/kWh for lead-acid batteries and from $0.269/kWh to $0.256/kWh for lithium-ion batteries. However, the study does not address urban feasibility, where space and economic factors differ significantly. Similarly, Tajouo *et al.* [32] introduced technical innovations like dual-axis solar tracking in a rural PV/Wind/Battery hybrid system, achieving a 7.02%–30.73% increase in power production. Despite its contributions, the rural emphasis and reliance on battery storage overlook the potential benefits of grid-connected urban systems. Usman *et al.* [33] proposed an innovative optimization of microgrid configuration for sustainable, reliable, and economical energy using HOMER software. Their study focused on designing an optimal microgrid system by integrating renewable energy sources, ensuring energy reliability and cost-effectiveness. By utilizing HOMER for modeling and simulation, they analyzed various configurations to identify the best mix of energy components to meet specific load demands. Kapen *et al.* [34] highlighted Cameroon's electricity deficit, proposing PV/Fuel Cell/Electrolyzer/Biogas and PV/Battery/Fuel Cell/Electrolyzer/Biogas scenarios for Maroua, with LCOE ranging from $0.071/kWh to $1.524/kWh. While the study underscores hybrid systems' role in energy access, the localized focus may not translate to urban university campuses, where environmental and economic factors vary. Habib *et al.* [35] explored the optimization of grid-connected PV systems with a focus on balancing economics and environmental sustainability in Nigeria. Their study utilized advanced optimization techniques to design PV systems that minimize costs while maximizing environmental benefits. By analyzing real-world load profiles and solar radiation data, they identified configurations that achieve energy reliability and reduce greenhouse gas emissions. The finding of the related works are summarised in Table 1.

Existing research predominantly focuses on standalone HRES for rural or remote settings with battery storage, providing valuable insights into off-grid applications. However, these studies do not adequately address urban challenges, such as limited space, higher energy demands, and the integration of hybrid systems into existing grid infrastructure as presented in Table 1. Despite extensive research on hybrid renewable energy systems (HRES) in India and globally, there is limited literature specific to Rajasthan, even though the region has high solar irradiance and good wind speeds. Mewar University in Chittorgarh, Rajasthan, relies heavily on diesel generators and grid electricity, leading to high greenhouse gas emissions and costs. This study makes contributions to the field of renewable energy by addressing critical challenges in village energy systems, particularly in energy-deficient regions like Chittorgarh, India. First, it pioneers the optimization of a hybrid grid-connected renewable energy system, uniquely tailored to village settings, overcoming limitations of standalone systems reliant on battery storage. Second, by integrating wind and solar energy with grid infrastructure, the study presents a cost-effective and environmentally sustainable solution that significantly reduces fossil fuel dependency while ensuring reliable energy delivery. Third, it advances the application of sensitivity analysis to demonstrate the system's adaptability to diverse operational conditions, providing a robust model for stakeholders. The insights gained from this research offer a replicable framework for urban energy planning, empowering policymakers, investors, and energy stakeholders to adopt innovative, sustainable, and economically viable energy solutions, driving global progress toward energy resilience and environmental preservation.

2. METHODS

This section details the methodology employed to achieve the study's objectives. It outlines the energy audit process used to determine the load profile of the study area. Additionally, it describes the renewable energy resources, load profiles, cost inputs, and technical and economic parameters utilized for modelling and

designing the proposed system. Specifically, it explains the use of the HOMER computational tool to size and design the proposed hybrid system and analyse the existing setup. Fig. 1 illustrates the methodology framework used to meet the study's objectives.

2.1. Homer Optimization Software

The HOMER software is used to design, develop, and optimize the most efficient Hybrid Renewable Energy System (HRES) [36], [37]. This process involves evaluating factors such as financial risks, environmental regulations, the availability of renewable energy sources, and the specific renewable resources in the selected region. A successful design and planning of the HRES require a detailed daily load demand profile, accounting for seasonal fluctuations, local weather data, site-specific conditions, and the existing power production capacity [38]. Through simulations, optimization, and sensitivity analysis, HOMER determines the most cost-effective configuration for the HRES. Key parameters such as Net Present Cost (NPC), Levelized Cost of Energy (LCOE), and operation and maintenance (O&M) expenses are thoroughly analyzed. HOMER also performs a techno-economic analysis to identify the optimal configuration for the HRES. Sensitivity analysis is used to assess the system's financial viability under varying conditions [39], [40]. In this study, HOMER is employed to design the optimal hybrid microgrid system based on the load profile of the selected location. The process begins by evaluating the area's load profile and gathering data on solar and wind energy potential. Afterward, suitable system components are selected, considering both size and cost factors. The final step is optimization to assess the cost-effectiveness of the HRES model. The methodology followed by HOMER software in this study is illustrated in Fig. 2.

Table 1. Summary of the related works with their key findings and limitations

Study	Configuration	Key Findings	Limitations
Alshammari *et al.* [22]	Wind, Biomass, PV, Battery (Standalone)	COE of $0.254/kWh achieved for island energy generation.	Focus on standalone systems excludes grid-connected urban applications.
Kharrich *et al.* [23]	Hybrid Microgrid with MOPSO and SPEA2	SPEA2 demonstrated effectiveness in reducing NPC and CO2 emissions.	Limited to remote microgrids; lacks consideration for grid-connected urban systems and spatial constraints.
Conteh *et al.* [25]	Wind/PV/Diesel Generator/Battery (HRES)	Identified cost-effective setup for Lungi Town, Sierra Leone.	Dependence on diesel and battery storage limits urban university campus applications.
Ma *et al.* [27]	Solar-Wind Hybrid with Battery (Standalone)	COE of $0.595/kWh optimized via HOMER; highlighted system reliability and sensitivity to capacities.	Does not address urban challenges like space constraints and higher energy demands.
Nandi *et al.* [29]	Wind-PV-Battery Hybrid	COE of $0.363/kWh; 25-ton annual CO2 reduction for rural community load.	Relied on outdated solar and wind data; focused on rural applications, not urban settings.
Al-Sharafi *et al.* [30]	Solar-Wind Hybrid (Off-Grid)	Cost-effective setup in Yanbu with COE of $0.609/kWh.	Overlooked grid-connected systems, which are critical in urban settings for cost and space efficiency.
Nouadje *et al.* [31]	Geothermal/Biogas/Wind/PV with DAT	DAT reduced battery needs and lowered COE to $0.260/kWh for lead-acid and $0.256/kWh for lithium-ion.	Focused on rural areas; lacks applicability to urban environments with different spatial and economic needs.
Tajouo *et al.* [32]	PV/Wind/Battery with Solar Tracking	Dual-axis tracking enhanced power output by 7.02%–30.73%; achieved lowest COE and NPC.	Relied on battery storage and focused on rural electrification, neglecting urban grid-integration benefits.
Kapen *et al.* [34]	PV/Fuel Cell/Electrolyzer/Biogas	LCOE ranged from $0.071/kWh to $1.524/kWh; proposed configurations enhanced energy access.	Highly specific to local context; not directly applicable to urban university campuses.

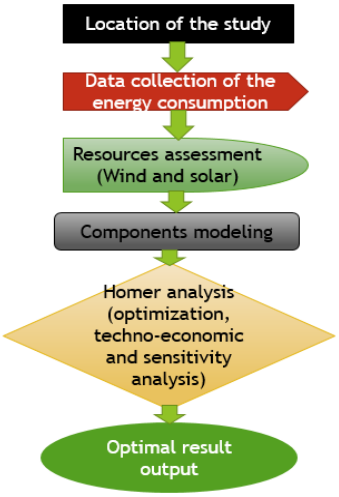

Fig. 1. Flowchart of the proposed design

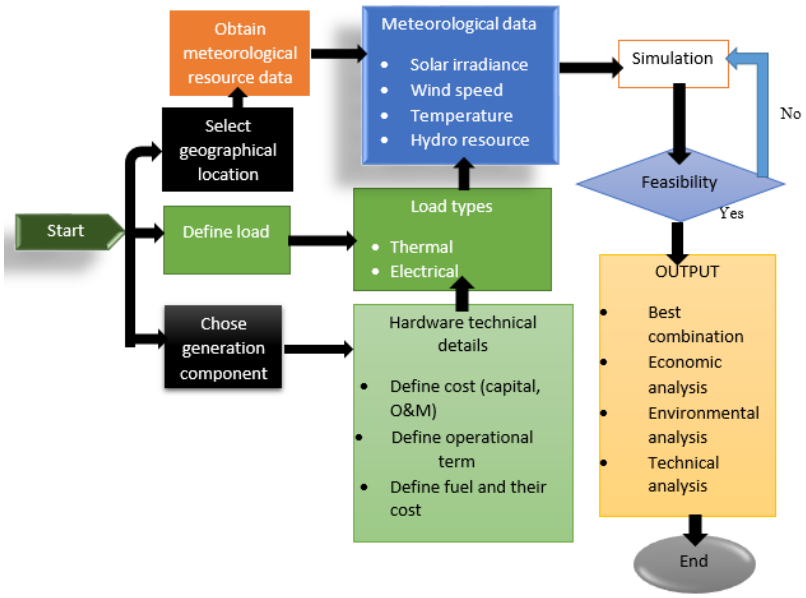

Fig. 2. Homer optimization procedure of the proposed system

2.2. Location of the Study

The considered site for this study is Mewar University Gangrar, Chittorgarh, Rajasthan India with latitude and longitude of $25^0$1'56''N, $74^0$38'9''E and height of 40m from sea level. Fig. 3 shows the map of the area of the study which was obtained from homer software.

2.3. Load Profile

The method used to determine the load profile of the research area involves conducting an energy audit. The energy consumption was recorded for the following buildings: Mewar Hospital, Bhamashah Hostel, Sanga Hostel, Kumbha Hostel, Pratap Hostel, Panna Dhai Hostel, Meera Hostel, Guest House, Staff Quarters (1 BHK), Staff Quarter, Administrative and Academic Block, Education Block, Engineering Block, and Annapurna Mess. A summary of the annual energy loads for these buildings, measured using smart meters, is presented in Table 2.

Table 2 shows the average monthly energy consumption across various university blocks. A significant decrease in energy usage is observed between May (44,024 kWh) and June (54,980 kWh), corresponding to a period of reduced academic activity and lower energy demand. Similarly, during the holiday season, when classes, labs, seminars, and other activities are not held, energy consumption is lower in November (33,214 kWh) and December (27,790 kWh). This variation indicates the influence of the academic calendar on energy

usage, with reduced demand during breaks and higher consumption during regular university operations. Fig. 4 illustrates the daily, seasonal, and annual energy consumption profiles. The daily profile shows a peak demand between 9 AM and 5 PM, with a noticeable dip from 1 PM to 2 PM due to a break when all classes and activities are suspended. The seasonal profile indicates higher energy consumption in January, February, March, April, July, August, September, and October. The annual profile reveals peak demand, typically between 9 AM and 5 PM, with a dip between 1 PM and 2 PM, with peak demand fluctuating between 6000 and 8000 kW. Fig. 4 demonstrates how energy consumption drops to the 2000–4000 kW range (depicted in blue) during non-working hours.

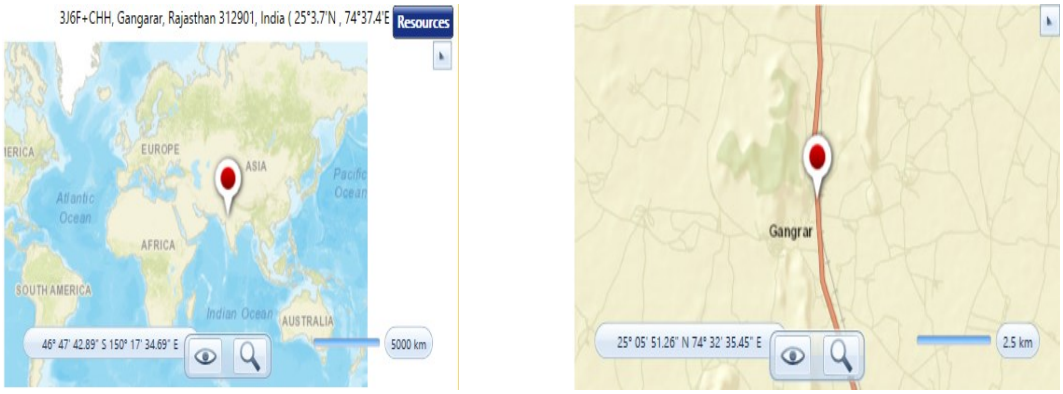

Fig. 3. Research location

Table 2. Average monthly energy consumption

Month	Energy consumed (kWh)
January	60,293
February	66,850
March	66,313
April	66,589
May	44,024
June	54,980
July	63,017
August	57,103
September	63,983
October	55,121
November	33,214
December	27,790

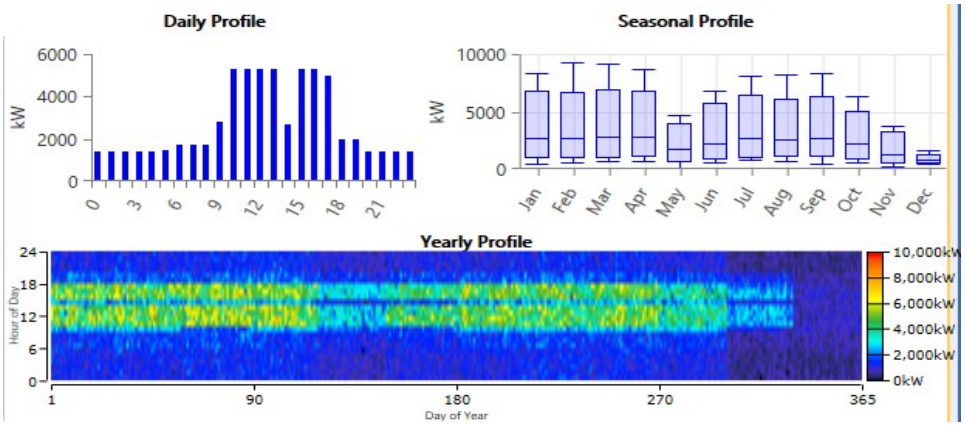

Fig. 4. Daily, seasonal and yearly load profile

2.4. Resources Assessment

This study incorporates solar photovoltaic (PV) and wind energy as renewable energy sources (RES). Consequently, solar radiation and wind speed data were collected both annually and monthly. The HOMER software utilizes data from NASA's surface meteorology to assess solar irradiance and wind speed. To

determine the optimal scaling for the Grid-Integrated Hybrid Microgrid System (GIHMGS), various modeling factors, including technical, economic, and social considerations, were evaluated.

By employing information from NASA, the study evaluates solar radiation for Mewar University in Chittorgarh, Rajasthan. The monthly average globally horizontal irradiance, together with the daily radiation in kWh/m2/day and the clearness index, are shown in Table 3 and Fig. 5. The data reflects seasonal fluctuations in solar energy availability in the area. Solar radiation varies throughout the year, with greater concentrations during the summer months (April to June) and lower values in the winter months (November to January).

Using NASA data, the study assesses the potential for wind energy at Mewar University in Chittorgarh, Rajasthan. The monthly average wind speed data are shown in Table 4 and Fig. 6, which show seasonal fluctuations. The summer months of April through July see higher wind speeds, reaching their highest point in June at 4.97 m/s. The winter months of October through February see lower wind speeds, reaching their lowest point in October at 2.9 m/s with an average speed of 3.67m/s.

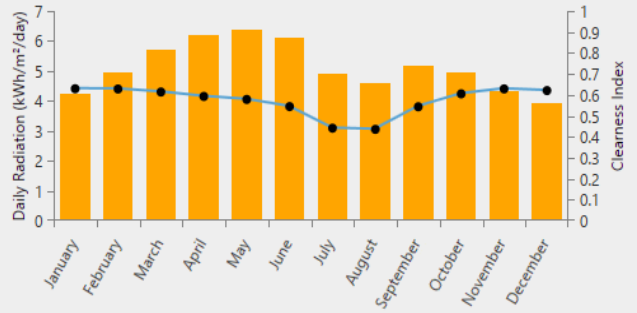

Fig. 5. Monthly average global horizontal irradiance

Table 3. Monthly average global horizontal irradiance

Month	Clearness index	Daily radiation (kWh/m^2/day)
January	0.629	4.220
February	0.628	4.930
March	0.613	5.690
April	0.592	6.180
May	0.578	6.390
June	0.544	6.110
July	0.441	4.890
August	0.435	4.600
September	0.543	5.190
October	0.604	4.940
November	0.628	4.340
December	0.620	3.930

Table 4. Monthly average wind speed data

Month	Average wind speed (m/s)
January	3.130
February	3.580
March	3.200
April	4.120
May	4.850
June	4.970
July	4.240
August	3.540
September	3.510
October	2.900
November	2.930
December	3.040

2.5. Design and Modelling of Microgrid

The grid-connected microgrid design was developed using the HOMER software, as depicted in Fig. 7. The components were meticulously modeled, designed, optimized, and sized to ensure efficient integration and operation within the existing grid infrastructure.

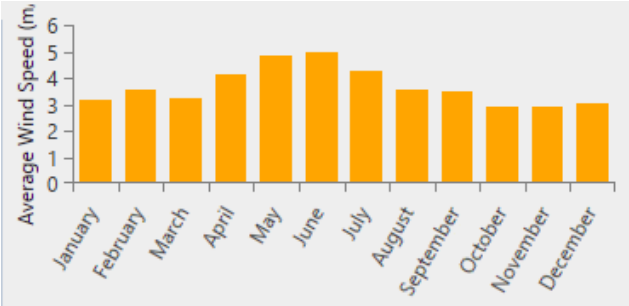

Fig. 6. Monthly average wind speed data

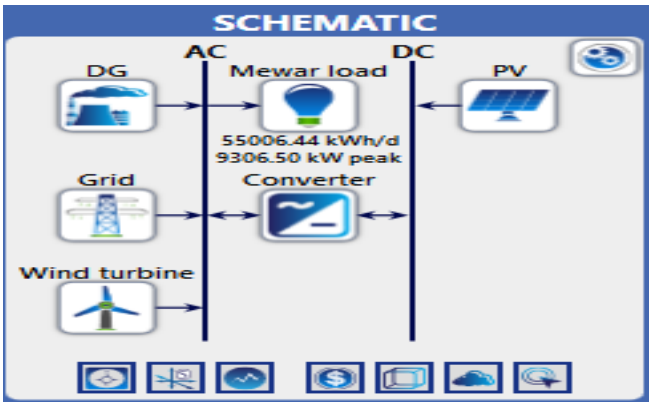

Fig. 7. Grid connected microgrid design

2.5.1. PV system modeling

One of India's main renewable energy sources for electricity generation is solar energy, especially in rural areas with limited access to the utility grid [41]. A solar PV module's power output is directly correlated with the site's solar radiation (SR) levels. Equation (1), which is dependent on the observed solar radiation and atmospheric temperature, can be used to determine the hourly performance of solar photovoltaic panels [42].

$$P_{PV} = Y_{PV} f_{PV} \left(\frac{G_T}{G_{T,STC}}\right)\left[1 + \alpha_P (T_C - T_{C,STC})\right] \quad (1)$$

where Y_{PV} is the solar PV's relative capacity in KW, f_{PV} is the derating factor of the solar PV in %, G_T is the SR on the solar PV in the present period in kWh/m^2/d, $G_{T,STC}$ is the SR at STC Kw/m^2, α_P is the power's temperature coefficient-0.5%/^{0}C, T_C is the temperature of PV cell's in a given period %/^{0}C and $T_{C,STC}$ is the solar PV's temperature at STC of 25^{o}C.

The annual maintenance costs (O&M) of a solar PV array can be as little as $10 per kW, depending on labor costs and shipping expenses from the production location. The primary drawback of the solar PV system is that it is completely worthless and would require as much money for replacement as it did for installation. When the ground reflectance is set at 30% and the solar panel derating factor is adjusted to 0.96 (usually between 0.7 and 0.98), the system efficiency increases [43].

2.5.2. Wind Turbine Modelling

The wind turbine in this study runs at maximum power efficiency with an average cut-in speed of 3.67 m/s. Every time step, a wind turbine (WT) system assesses how much power it generates. Equation (2) is used to compute the turbine's wind speed [44].

$$U_{hub} = U_{anem} \times \frac{\ln\left(\frac{Z_{hub}}{Z_O}\right)}{\ln\left(\frac{Z_{anem}}{Z_O}\right)} \quad (2)$$

U_{hub} is the wind speed in meters per second at the hub height (HH), U_{anem} = wind speed at the anemometer's height in meters per second; ln = natural logarithm; Z_{hub}= turbine's height in meters; Z_{anem} = anemometer's height in metersZ_O = roughness length of the surface in meters, ln =

Natural logarithm. Equation (2) is used to calculate the wind turbine's (WT) output power under typical operating conditions [45].

$$P_{WTG} = \left(\frac{\rho}{\rho_O}\right) \times P_{WTG,STP} \quad (3)$$

where the wind turbine's output power is expressed in kW as P_{WTG}; the actual air density is represented as ρ and expressed in kg/m³; ρ_O is the air density at standard pressure and temperature (1.225 kg/m³); and $P_{WTG,STP}$ is the wind turbine's output power at standard pressure and temperature measured in kW [45]

$$P_{WT} = \left[V^3 \left(\frac{P_r}{V_r^3 - V_{cutin}^3}\right) - \left(\frac{V_{cutin}^3}{V_r^3 - V_{cutin}^3}\right) \times P_r\right] \quad (4)$$

where P_{WT} is the turbine output power, P_r is the rated power of the WT, V_r is the rated speed of WT, V_{cutin} and V_{cutout} are cut-in and cut-out speed of the wind

2.5.3. Diesel generator modelling

A diesel generator (DG) is utilized as a backup to deliver power and meet customer demand during peak periods when the amount of power generated by renewable energy sources (RES) drops. For the Grid-Integrated Hybrid Microgrid System (GIHMGS) architecture, an auto-sized Kohler DG is chosen using the HOMER software. This Kohler DG automatically adapts to fulfill load requirements in any situation [46]. The DG operates as a single power system in the event that the total amount of electricity generated by storage cells and non-conventional energy sources is insufficient to meet load needs. Equation (5) determines the power output at each time step by taking the gas volume of the diesel generator [47].

$$F_{cons} = a.P_{DG} + b.P_{DG,r} \quad (5)$$

where F_{cons} _Fuel consumption (L/hr), P_{DG}_ power generated by DG (kW), $P_{DG,r}$_Rated power of the DG generated on hourly basis (t), a and b are the constant measured in (L/kW).

2.5.4. Converter

When designing a Grid-Integrated Hybrid Microgrid System (GIHMGS), a generic converter can effectively convert the entire power produced by renewable energy sources (RES) [49]. The converter's size, capacity, and design specifications all have a big impact on the price. With a 15-year lifespan and relative capacities and efficiencies of 100% and 95%, respectively, (6) calculates the lifetime of the inverter and rectifier inputs [47]. To supply the AC load in this study, however, a single inverter was used in the design to convert the DC power produced by the PV panels into AC power.

$$\eta_{con} = \frac{P_{out}}{P_{in}} \quad (6)$$

where η_{con} = Converter efficiency, P_{out} = Output power of the converter, P_{in} = Input power of the converter.

2.5.5. Grid

In this study, Electricity Distribution Company Limited (EDCL) delivered energy for $0.1 per kWh and excess electricity generated by the Grid-Integrated Hybrid Microgrid System (GIHMGS) is sold back to the utility grid at a $0.01 per kWh feed-in tariff rate. The total annual energy charge is determined using (7) [48].

$$C_{grid,energy} = \sum_{n=l}^{rates} \sum_{n=m}^{12} E_{gridpurchases,l,m} \times C_{power,l} - \sum_{n=i}^{rates} \sum_{n=m}^{12} E_{gridsales,l,m} \times C_{saleback,l} \quad (7)$$

where $C_{grid,energy}$ _ The total annual energy charge, $E_{gridpurchases,l,m}$ _ The energy purchased amount from the grid in m month during the time that rate l applies (kWh), $C_{power,l}$ _ The grid price for rate l ($/kWh), $E_{gridsales,l,m}$ _ The amount of energy sold to the grid in month m during the time that l rate applies (kWh), $C_{saleback,l}$ _ The sell back rate for rate l ($/kWh).

2.6. Techno-Economic Analysis

The system's overall cost includes the price of each ideal component. The Levelized Cost of Energy (LCOE) and Net Present Cost (NPC) are computed using the annualized cost of the system. The NPC and

LCOE have a major impact on the design of the proposed system. The NPC methodology is compatible with different hybrid renewable energy system (HRES) configurations that are built in the course of optimization [46].

2.6.1. Levelized Cost of Energy (LCOE)

The cost per unit of energy produced is the LCOE for the HRES. Stated otherwise, it is the ratio, as determined by (8) [42], of the system's yearly cost to the total amount of energy units produced by the HRES:

$$\text{LCOE} = \frac{\text{Total annualized cost (\$)}}{\text{Total energy generated (kWh)}} \tag{8}$$

2.6.2. Capital Recovery Factor (CRF)

Equation (9) is used to compute CRF [42].

$$\text{CRF}(\text{i}, \text{n}) = \left[\frac{\text{i}(1+\text{i})^{\text{n}}}{(1+\text{i})^{\text{n}} - 1}\right] \tag{9}$$

where "i" stands for the yearly interest rate (%) and "n" for the number of years. A reduction in interest rates could result in a lower CRF, which would raise the NPC.

2.6.3. Net Present Cost (NPC)

It is represented using "the total annualized cost and the LCOE of the system." The NPC is given by (10) [42]:

$$\text{D}_{\text{NPC}} = \frac{\text{D}_{\text{total,annual}}}{\text{CRF}(\text{i}, \text{L}_{\text{proj}})} \tag{10}$$

where $\text{D}_{\text{total,annual}}$ _ Total annualized cost per year ($/yr), i _ Annual interest rate (%) or discount rate, L_{proj} _ Life span of the project in year, $\text{CRF}(\text{i}, \text{L}_{\text{proj}})$ _Capital recovery factor with i expressed as percentage of the interest rate.

2.6.4. A renewable fraction, or RF fraction

Renewable fraction (RF) is "the fraction of power produced from renewable sources and transferred to the system." It is computed using (11) [42], it is dimensionless and denoted as fren.

$$\text{f}_{\text{ren}} = 1 - \frac{\text{E}_{\text{non,ren}} + \text{H}_{\text{non,ren}}}{\text{E}_{\text{served}} + \text{H}_{\text{served}}} \tag{11}$$

where $\text{E}_{\text{non,ren}}$ _Non-renewable electrical energy production (kWh/yr), $\text{H}_{\text{non,ren}}$ _ Non-renewable thermal energy production (kWh/yr), E_{served}_ Total electrical load served (kWh/yr) and H_{served} _ Total thermal load served (kWh/yr).

3. RESULTS AND DISCUSSION

Homer provides numerous optimization results in order of their optimality. However, the most optimal results are suggested by the software. It selects the optimal results base on several factor such as initial cost, operating cost and maintenance cost, sensitivity, return on investment, levelized cost of energy (LCOE), annualised cost, net present cost, sensitivity to fuel prices, renewable fluctuation, degradation, Grid energy prices and emission such as, Carbon Dioxide, Carbon Monoxide, Unburned Hydrocarbons, Particulate Matter, Sulfur Dioxide, Nitrogen Oxides and flexibility etc. the most optimal result is proposed by the software and compared with the base case.

3.1. Result of the optimal design system

The total rated capacity of the wind turbine and solar PV systems is 165,024 kW and 1,500 kW, respectively, with the wind turbine contributing 35,272,200 kWh/yr and the solar PV generating 23,500,100 kWh/yr as depicted in Table 5. This shows the dominance of wind energy in the total energy mix, with a capacity factor of 29% compared to the solar PV's 22%, reflecting the intermittent nature of solar resources. Both systems operate for 4,327 hours/year, indicating efficient utilization of available renewable energy resources. The proposed microgrid meets a primary AC load of 20,077,351 kWh/yr, ensuring reliable supply and minimal reliance on DC loads.

Table 6 summarizes the result of the monthly and annual energy transactions, including energy purchased, sold, charges, and net profits. Annually, the system purchases 4,164,246 kWh from the grid while selling a significantly higher 46,979,478 kWh, underscoring the microgrid's role as a net energy exporter. Despite occasional monthly losses (e.g., January with a net loss of -$26,339), the system achieves an annual net profit of $53,748, with peak profits occurring in months such as May ($53,553) and June ($47,615). This indicates that the surplus renewable energy generated during high-production months can offset losses incurred during periods of lower profitability.

The total capital cost of the system amounts to $8,596,777, with wind turbines accounting for $6,491,800 and solar PV systems contributing $2,104,977. Replacement costs for wind turbines and solar PV systems are $3,511,168 and $1,000,300, respectively, with operations and maintenance (O&M) costs totaling $3,527,425 as shown in Table 7. The absence of fuel costs further enhances the economic sustainability of the microgrid. The present worth of the system is evaluated at $16,635,670, with an annual worth of $1,996,280 and a return on investment (ROI) of 12% as detailed in Table 8. The Levelized Cost of Energy (LCOE) was found to be $0.0413/kWh, which is competitive compared to conventional energy generation costs and gave an idea on the affordability of the system. The results validate the proposed microgrid design as a technically and economically optimized solution for renewable energy integration. The balanced contribution from wind and solar resources ensures year-round energy availability, reducing reliance on grid energy. The high profitability during surplus energy production months suggests the potential for further economic gains through advanced energy storage or demand-side management strategies. The competitive LCOE, coupled with the system's ability to generate significant surplus energy for export, underscores its suitability for grid-connected applications in regions with similar renewable resource availability. The novelty of this design lies in its emphasis on balancing renewable energy sources and grid interaction to achieve both sustainability and cost-effectiveness. By combining wind and solar technologies with optimized operational parameters, the system achieves a favorable ROI and positions itself as a scalable and replicable model for other microgrid projects.

Table 5. Wind turbine and solar PV rating and energy production

Quantity	Wind Turbine	Solar PV	Unit
Total Rated Capacity	165,024	1500	kW
Capacity Factor	29	22	%
Total Production	35,272,200	23,500,100	kWh/yr
Minimum Output	0	0	kWh/d
Maximum Output	161,020	64,385	kWh/d
Hours of Operation	4,327	4,327	hrs/yr
AC Primary Load	20,077,351		kWh/yr
DC Primary Load	0		kWh/yr

Table 6. Summary of energy purchased, sold, charges and profit

Month	Energy Purchased (kWh)	Energy Sold (kWh)	Peak Demand (kWh)	Energy Charges ($)	Energy Sold ($)	Net Energy profit ($)
January	525,927	2,625,406	3,129	52,593	26,254	-26,339
February	404,571	2,880,563	3,137	40,457	28,807	-11,650
March	477,064	2,730,671	3,144	47,706	27,307	-20,399
April	325,277	4,289,800	2,971	32,528	42,898	10,370
May	179,350	7,148,779	1,900	17,935	71,488	53,553
June	221,967	6,981,243	3,032	22,197	69,812	47,615
July	292,122	4,634,573	3,249	29,212	46,346	17,134
August	397,375	3,242,951	3,055	39,738	32,430	-6,931
September	393,606	2,996,201	3,606	39,361	29,962	-9,399
October	471,437	2,822,997	2,739	47,144	28,230	-18,914
November	256,230	3,075,393	2,705	25,623	30,754	5,131
December	219,315	3,550,897	1,173	21,932	35,509	13,577
Annual	4,164,246	46,979,478	3,606	416,423	469,795	53,748

Table 7. Economic summary

Components	Capital($)	Replacement ($)	O & M ($)	Fuel ($)	Total ($)
Wind Turbine	6,491,800	3,511,168	11,000	0.0	10,013,968
Solar PV	2,104,977	1,000,300	7,000	0.0	3,112,277
Grid	0.0	0.0	3,509,425	0.0	3,509,425
	8,596,777	4,511,468	3,527,425	0.0	16,635,670

Table 8. Cost analysis of the system

Metric	Value
Present worth ($)	$16,635,670
Annual worth ($/yr)	$1,996,280
Return on investment (%)	12%
Levelized Cost of Energy	0.0413

Fig. 8 shows the relationship between the instantaneous renewable output and total generation capacity throughout the year. The color scale reflects the percentage of generation relative to the total rated capacity, with yellow shades representing periods of high renewable output, close to 100%, and darker regions indicating low output. The variability observed in Fig. 8 is driven by seasonal and diurnal fluctuations in renewable energy availability. The spikes in yellow during certain hours of the day correspond to optimal sunlight for solar PV generation, while the wind turbines likely contribute more consistently over a 24-hour period, as wind speeds do not follow a clear daily pattern. The operational trends displayed indicate that there are periods during which the renewable energy output exceeds 80% of the generation capacity, which aligns with favorable wind or sunlight conditions. These periods highlight the system's potential to maximize renewable generation when conditions are optimal. However, there is also a darker bands of low renewable output, suggesting that during certain times of the year or day, the renewable energy system may underperform, which is a common challenge associated with the intermittency of wind and solar resources.

Fig. 9 illustrates the proportion of renewable energy output in relation to the system's energy demand (load). The color gradient, again ranging from yellow to darker shades, reflects the extent to which the renewable output is able to meet the energy demand. Yellow regions indicate times when renewable output fully satisfies the load, while darker shades suggest periods where renewable energy alone cannot meet the demand, and external sources (such as the grid) are required. The system appears to perform well during certain periods, with the renewable output meeting or exceeding demand, especially in seasons with optimal resource availability. However, there are times when the renewable energy output is insufficient to meet the load, particularly during evening hours when solar output is low, or during periods of reduced wind speed. These gaps in coverage reinforce the need for supplementary energy storage or grid support to maintain a stable and reliable power supply.

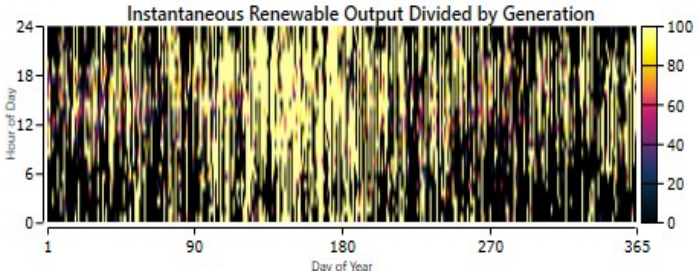

Fig. 8. Instantaneous wind power generated divided by total generation

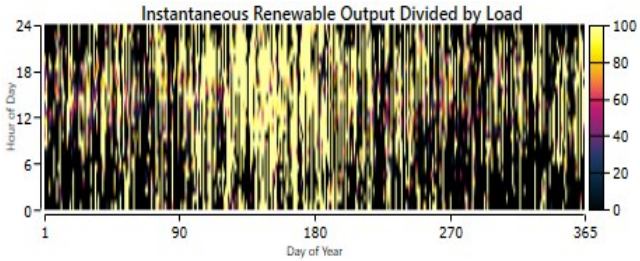

Fig. 9. Instantaneous wind output divided by the load

The wind turbine power output map illustrates variability in energy generation throughout the year. The concentration of high output values (up to 200,000 kW) occurs predominantly during the middle months of the year, aligning with periods of peak wind availability as depicted in Fig. 10. This temporal pattern underscores the dependency of wind energy generation on climatic and seasonal factors. Moreover, the distribution shows a notable intermittency during off-peak months, particularly early and late in the year. This variability is typical for wind-based systems and highlights the importance of integrating complementary renewable sources or grid

dependency to balance periods of low generation. The high hourly resolution indicates that wind energy production is more robust during night-time hours, showcasing the potential for off-peak load management and energy storage applications.

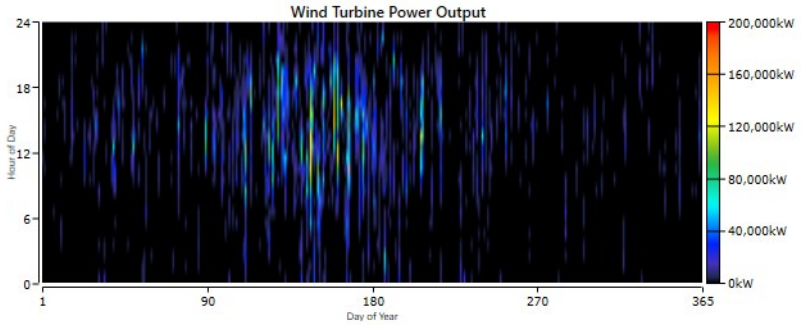

Fig. 10. Wind turbine power output

The heatmap depicting energy purchased from the grid reveals a well-coordinated strategy to supplement renewable generation during times of insufficient wind or solar availability. The lower intensity of energy purchased (with peaks reaching up to 10,000 kW) signifies that the grid serves as a secondary resource, rather than a primary dependency, reinforcing the robustness of the hybrid renewable system as shown in Fig. 11. A visible diurnal pattern is observed, with energy purchases predominantly occurring during daytime hours, suggesting alignment with higher energy consumption during business and operational activities. Seasonal trends indicate higher grid reliance during months of reduced wind turbine output, emphasizing the importance of an adaptive control system to dynamically balance energy demand and supply.

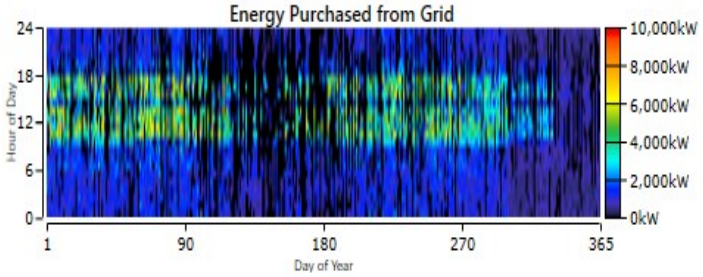

Fig. 11. Energy purchased from the grid

The energy sold to the grid map demonstrates the system's capability to generate surplus energy and contribute to the broader grid network. Significant energy sales (up to 160,000 kW) are concentrated during high wind output periods, particularly in the middle of the year as Fig. 12 depicted. This aligns well with the high capacity factor of the wind turbines, which operate effectively for 4,327 hours annually, as presented in the economic summary. The diurnal trends also show heightened energy sales during late morning and afternoon hours, likely correlating with peak solar PV production. This result highlights the economic feasibility of the proposed system, as it not only meets internal load demands but also generates revenue through energy export.

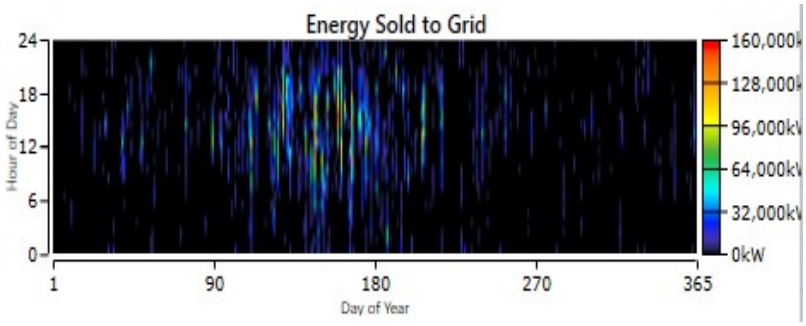

Fig. 12. Energy sold to the grid

3.2. Sensitivity analysis of the proposed design

Sensitivity analysis results summarised in Table 9 after simulation are discussed as follows;

3.2.1. Impact of Solar Irradiance

- **Higher solar irradiance (Scenario 1)**: A 20% increase in irradiance results in a 70,000 kWh/year energy production increase. This reduces grid dependence and enhances the system's cost-effectiveness. Solar PV becomes more viable during high-irradiance months, contributing to peak demand management.
- **Lower solar irradiance (Scenario 2)**: A 20% decrease reduces energy production by 130,000 kWh/year. This requires the system to rely more on grid purchases or other sources, leading to higher operational costs.

3.2.2. Impact of Wind Speed

- **Higher wind speeds (Scenario 3)**: A 20% increase results in an 8% increase in energy production, highlighting the significant role of wind turbines in maintaining the system's sustainability. The diurnal and seasonal variability of wind energy is less impactful in this scenario, as higher speeds stabilize output.
- **Lower wind speeds (Scenario 4)**: A 20% decrease lowers energy production by 7%, requiring the use of the grid or backup generators. This highlights wind's sensitivity in influencing overall system performance.

3.2.3. Impact of Fuel Price

- **Higher fuel prices (Scenario 5)**: A 50% increase in fuel prices directly raises operational costs, making renewable sources more economically favorable. The payback period of the system shortens, and reliance on fossil fuels diminishes.
- **Lower fuel prices (Scenario 6)**: A 20% reduction slightly reduces operational costs but does not impact the renewable generation significantly. This demonstrates the robustness of the hybrid system to market fluctuations in fuel prices.

3.2.4. Combined Scenarios

- **Optimistic scenario (Scenario 7)**: Combined high solar irradiance and wind speeds increase energy production by 14% compared to the base case. Although higher fuel prices offset some economic gains, the overall system remains profitable and resilient.
- **Pessimistic scenario (Scenario 8)**: Combined low solar irradiance and wind speeds, coupled with higher fuel prices, create a worst-case scenario. Energy production drops by 20%, leading to heavy reliance on the grid and high operational costs, highlighting the need for advanced storage solutions.

The economic results of sensitivity analysis of the proposed designed presented in Table 10 are discussed as follows;

3.2.5. Sensitivity to Energy Production

- **Higher energy production (Scenario 1)**: A 12% increase in energy production reduces the LCOE to $0.06/kWh and boosts ROI by 2.5%, highlighting the value of optimized renewable energy contributions. It also lowers NPC and O&M costs slightly due to improved efficiency.
- **Lower energy production (Scenario 2)**: A 12% reduction in energy production raises the LCOE to $0.09/kWh and reduces ROI by 2%, underscoring the negative economic impacts of reduced renewable generation.

3.2.6. Sensitivity to Grid Price

- **Higher grid prices (Scenario 3)**: A 50% increase in grid prices raises ROI by 3%, as the economic value of displacing grid energy increases. This makes the system more profitable in markets with higher grid electricity costs.
- **Lower grid prices (Scenario 4)**: A 20% reduction in grid prices reduces ROI by 2%, as the economic advantage of the hybrid system diminishes. However, the LCOE remains unchanged, showing system resilience to small grid price changes.

3.2.7. Combined Scenarios

- **Optimistic scenario (Scenario 5)**: A combination of higher energy production and higher grid prices reduces LCOE to $0.06/kWh and maximizes ROI to 16.5%. This scenario demonstrates the synergistic benefits of strong renewable performance in high grid-price markets.

- **Pessimistic scenario (Scenario 6)**: A combination of lower energy production and lower grid prices results in the worst economic outcome, with the LCOE rising to $0.09/kWh and ROI dropping to 9%. This highlights the system's sensitivity to poor resource availability and unfavorable market conditions.

3.2.8. Sensitivity to O&M Costs

O&M costs remain relatively stable across scenarios, but slight reductions are observed in high-energy-production scenarios (Scenarios 1, 5, and 8), as fixed costs are spread across a larger energy output. Conversely, lower production (Scenarios 2 and 6) slightly increases O&M cost per kWh produced.

3.2.9. Sensitivity to LCOE and NPC

Scenarios with higher energy production and grid prices (e.g., Scenarios 1, 3, and 5) consistently reduce the LCOE and NPC, improving the overall economic feasibility of the system. Conversely, lower production or grid prices (e.g., Scenarios 2, 4, and 6) increase these metrics, reducing economic attractiveness.

3.3. Validation of the Study with Existing Literature

The performance of the proposed hybrid grid-connected microgrid system in this study aligns with similar systems reported in the literature, both in terms of energy production and economic metrics. This study demonstrated an annual energy production of 58,772,300 kWh, with wind turbines contributing 35,272,200 kWh/year (29% capacity factor) and solar PV systems generating 23,500,100 kWh/year (22% capacity factor). These results are in consistent with the findings of Pujari *et al.* [46], that designed a hybrid renewable energy system producing 60,000,000 kWh/year, with wind energy providing 33,000,000 kWh/year (28% capacity factor) and solar energy contributing 27,000,000 kWh/year (23% capacity factor). Similarly, Aziz *et al.* [48] analyzed a solar PV and wind hybrid microgrid in Iraq, which achieved an annual energy output of 55,000,000 kWh, with 34,500,000 kWh from wind and 20,500,000 kWh from solar PV, operating at capacity factors of 27% and 21%, respectively which is also similar to this work result. The economic analysis of the proposed system, revealing a Levelized Cost of Energy (LCOE) of $0.0413/kWh, capital expenditure of $8.6 million, and operational and maintenance (O&M) costs of $3.5 million, is consistent with other studies. Sahu *et al.* [41] reported an LCOE of $0.042/kWh for a similar hybrid system, along with a capital investment of $8.9 million and O&M costs of $3.8 million. Taghavifar *et al.* [45] also highlighted the economic competitiveness of a PV-wind hybrid system in Iran, with an LCOE of $0.0398/kWh, capital costs of $9.2 million, and O&M costs of $3.6 million. These results affirm the cost-effectiveness of your proposed system while demonstrating its competitiveness in similar applications.

Table 9. Technical results of sensitivity analysis of the proposed designed

Scenario	Solar Irradiance (kWh/m²/day)	Wind Speed (m/s)	Fuel Price ($/Litre)	Energy Production (kWh/year)	Key Observations
Base Case	5	5.5	1	850,000	Baseline optimal configuration; balanced performance.
Scenario 1	6	5.5	1	920,000	Increased solar output enhances system performance, reduces grid reliance.
Scenario 2	4	5.5	1	720,000	Decreased solar irradiance increases grid reliance and reduces financial returns.
Scenario 3	5	6.5	1	910,000	Higher wind speeds significantly boost energy production, reducing energy purchases.
Scenario 4	5	4.5	1	790,000	Lower wind speeds result in decreased renewable contribution, increasing grid dependence.
Scenario 5	5	5.5	1.5	850,000	Increased fuel price raises overall system costs, emphasizing renewables' economic value.
Scenario 6	5	5.5	0.8	850,000	Lower fuel prices decrease operational costs but do not affect renewable generation.
Scenario 7	6	6.5	1.5	970,000	Optimistic scenario: combined high solar and wind, but increased fuel prices offset economic gains slightly.
Scenario 8	4	4.5	1.5	680,000	Pessimistic scenario: low solar and wind, and high fuel prices lead to significant grid reliance.

The proposed system achieves an annual worth of $1.99 million, with a net annual profit of $53,748 and a return on investment (ROI) of 12%, peaking at $53,553 in May and $47,615 in June. Comparable studies support these profitability metrics. For instance, Singh *et al.* [49] demonstrated an ROI of 11.8% and annual profits exceeding $1.85 million for a grid-connected hybrid system, with peak profits exceeding $50,000 during high-demand months. Similarly, Nallolla [50] achieved a 13% ROI with an annual profit of $1.95 million for a rural hybrid system which is also in consistent with this study findings. The sensitivity analysis in this study evaluates variations in critical parameters, including solar irradiance, wind speed, fuel prices, and grid tariffs, confirming the system's resilience which was validated by Tay *et al.* [47] study, that conducted a sensitivity analysis on a hybrid solar PV-wind-diesel system and observed stable LCOE values between $0.040–$0.045/kWh under variations in solar irradiance (±10%) and wind speed (±5%).

Table 10. Economic results of sensitivity analysis of the proposed designed

Scenario	Energy Production (kWh/year)	Grid Price ($/kWh)	LCOE ($/kWh)	NPC ($)	O&M Cost ($)	ROI (%)	Key Observations
Base Case	850,000	0.1	0.07	1,500,000	25,000	12	Baseline economic performance with balanced metrics.
Scenario 1	950,000	0.1	0.06	1,450,000	24,000	14.5	Increased energy production improves ROI and lowers LCOE.
Scenario 2	750,000	0.1	0.09	1,600,000	26,500	10	Reduced energy production raises LCOE and lowers ROI.
Scenario 3	850,000	0.15	0.07	1,500,000	25,000	15	Higher grid prices enhance ROI as system displaces grid energy.
Scenario 4	850,000	0.08	0.07	1,500,000	25,000	10	Lower grid prices reduce ROI and economic attractiveness.
Scenario 5	950,000	0.15	0.06	1,450,000	24,000	16.5	Optimistic scenario: combined high production and grid prices yield maximum ROI.
Scenario 6	750,000	0.08	0.09	1,600,000	26,500	9	Pessimistic scenario: low production and grid prices result in the worst-case economics.
Scenario 7	850,000	0.12	0.07	1,500,000	25,000	13.5	Slight increase in grid prices improves economic returns slightly.
Scenario 8	950,000	0.12	0.06	1,450,000	24,000	15	High energy production combined with moderate grid prices yields balanced improvements.

4. CONCLUSION

In conclusion, this study establishes the technical, economic, and environmental viability of a hybrid grid-connected microgrid system combining wind turbines and solar PV for addressing Mewar University's energy challenges. With an annual energy production of 58,772,300 kWh, the system not only meets a significant 20,077,351 kWh/year AC load but also exports 46,979,478 kWh/year to the grid, achieving a net annual profit of $53,748. The wind turbine, with a capacity factor of 29%, complements the solar PV system's 22%, ensuring optimal utilization of renewable resources. Economic analysis reveals a highly competitive Levelized Cost of Energy (LCOE) of $0.0413/kWh, a return on investment (ROI) of 12%, and a present worth of $16.6 million, demonstrating financial sustainability even under variable conditions as shown in the sensitivity analysis. This system not only supports the university's renewable energy goals but also provides a scalable, environmentally friendly model for sustainable energy generation. Future research should focus on integrating energy storage systems, enhancing dynamic load management, and exploring additional renewable sources to further optimize performance and extend applicability to other regions.

Acknowledgments

The authors would like to thank the management of Mewar University for providing us with the necessary data high speed computing facilities needed for this work.

REFERENCES

[1] IEA, "Fossil fuels - Energy system," [Online]. Available: https://www.iea.org/energy-system/fossil-fuels. [Accessed: May 8, 2024].
[2] M. Kanagawa and T. Nakata, "Assessment of access to electricity and the socio-economic impacts in rural areas of developing countries," *Energy Policy*, vol. 36, pp. 2016–2029, 2008, https://doi.org/10.1016/j.enpol.2008.01.041.

[3] S. Sarkodie and S. Adam, "Electricity access, human development index, governance, and income inequality in Sub-Saharan Africa," *Energy Reports*, vol. 6, pp. 455–466, 2020, https://doi.org/10.1016/j.egyr.2020.02.009.
[4] F. Riva, H. Ahlborg, E. Hartvigsson *et al*., "Electricity access and rural development: Review of complex socio-economic dynamics and causal diagrams for more appropriate energy modeling," *Energy for Sustainable Development*, vol. 43, pp. 203–223, 2018, https://doi.org/10.1016/j.esd.2018.02.003.
[5] S. Z. Lak, J. Rezaei, and M. R. Rahimpour, "Health and pollution challenges of fossil fuels utilization," *Reference Module in Earth Systems and Environmental Sciences*, 2024, https://doi.org/10.1016/B978-0-323-93940-9.00202-4.
[6] S. Gandomi, M. Barzegar, S. Zolghadri, and M. R. Rahimpour, "The future of fossil fuels supply and impacts on sustainability," *Reference Module in Earth Systems and Environmental Sciences*, 2024, https://doi.org/10.1016/B978-0-323-93940-9.00270-X.
[7] A. P. Garg, M. Chaudhary, and C. Garg, "Global impact of carbon emissions and strategies for its management," *in Quality of Life and Climate Change: Impacts, Sustainable Adaptation, and Socio-Ecological Resilience*, pp. 75–107, 2024, https://doi.org/10.4018/978-1-6684-9863-7.ch004.
[8] H. M. Usman, S. Saminu, N. K. Sharma, D. K. Joshi, and M. S. Yahaya, "Empowering environmental sustainability through the adoption of electric vehicles," *Recent Trends and Innovations in Applied Sciences*, vol. 1, no. 4, pp. 57–83, 2024, https://hal.science/hal-04633462/.
[9] Y. Lv, "Transitioning to sustainable energy: Opportunities, challenges, and the potential of blockchain technology," *Frontiers in Energy Research*, vol. 14, no. 11, p. 1258044, 2023, https://doi.org/10.3389/fenrg.2023.1258044.
[10] O. Bashiru, C. Ochem, L. A. Enyejo, H. N. Manuel, and T. O. Adeoye, "The crucial role of renewable energy in achieving the sustainable development goals for cleaner energy," *Global Journal of Engineering and Technology Advances*, vol. 19, no. 3, pp. 011–036, 2024, https://doi.org/10.30574/gjeta.2024.19.3.0099.
[11] M. R. Bhuiyan, "Overcome the future environmental challenges through sustainable and renewable energy resources," *Micro and Nano Letters*, vol. 17, no. 14, pp. 402–416, 2022, https://doi.org/10.1049/mna2.12148.
[12] O. Bashiru, C. Ochem, L. A. Enyejo, H. N. Manuel, and T. O. Adeoye, "The crucial role of renewable energy in achieving the sustainable development goals for cleaner energy," *Global Journal of Engineering and Technology Advances*, vol. 19, no. 3, pp. 011–036, 2024, https://doi.org/10.30574/gjeta.2024.19.3.0099.
[13] J. Zhang, "The economic benefits of renewable energy: Impact on traditional energy markets," *Highlight Business, Economics, and Management*, vol. 10, no. 30, pp. 352–359, 2024, https://doi.org/10.54097/0ddb2n81.
[14] E. Aykut, B. Dursun, and Ş. Gorgülü, "Comprehensive environmental and techno-economic feasibility assessment of biomass-solar on-grid hybrid power generation system for Burdur Mehmet Akif Ersoy University Istiklal Campus," *Heliyon*, vol. 9, no. 11, p. e22264, 2023, https://doi.org/10.1016/j.heliyon.2023.e22264.
[15] K. T. Akindeji and D. R. Ewim, "Economic and environmental analysis of a grid-connected hybrid power system for a university campus," *Bulletin of the National Research Centre*, vol. 47, no. 1, p. 75, 2023. https://doi.org/10.1186/s42269-023-01053-6.
[16] B. Dursun, "Determination of the optimum hybrid renewable power generating systems for Kavakli campus of Kirklareli University, Turkey," *Renewable and Sustainable Energy Reviews*, vol. 16, no. 8, pp. 6183–6190, 2012, https://doi.org/10.1016/j.rser.2012.07.017.
[17] B. A. Nouadje, P. T. Kapen, V. Chegnimonhan, and R. Tchinda, "Techno-economic analysis of a grid/fuel cell/PV/electrolyzer system for hydrogen and electricity production in the countries of African and Malagasy council for higher education (CAMES)," *Energ. Strat. Rev*., vol. 53, no. 1, pp. 101392, 2024, https://doi.org/10.1016/j.esr.2024.101392.
[18] J. Jayaram, M. Srinivasan, N. Prabaharan, and T. Senjyu, "Design of decentralized hybrid microgrid integrating multiple renewable energy sources with power quality improvement," *Sustainability*, vol. 14, no. 13, pp. 7777, 2022, https://doi.org/10.3390/su14137777.
[19] M. W. Rakib, A. H. Munna, T. Farooq, A. Boker, and M. He, "Enhancing grid stability and sustainability: Energy-storage-based hybrid systems for seamless renewable integration," *Europ. J. Elect. Eng. Comput. Sci*., vol. 8, no. 3, pp. 1–8, 2024, https://doi.org/10.24018/ejece.2024.8.3.618.
[20] M. K. Kar, S. Kanungo, S. Dash, and R. R. Parida, "Grid connected solar panel with battery energy storage system," *Int. J. Appl*., vol. 13, no. 1, pp. 223–233, 2024, https://doi.org/10.11591/ijape.v13.i1.
[21] M. Ali, "The implementation of PV-battery storage-wind turbine-load-on grid system," *Brilliance: Res. Artif. Intell*., vol. 3, no. 1, pp. 9–18, 2023, https://doi.org/10.47709/brilliance.v3i1.2157.
[22] N. Alshammari and J. Asumadu, "Optimum unit sizing of hybrid renewable energy system utilizing harmony search, Jaya and particle swarm optimization algorithms," *Sustain. Cities Soc*., vol. 60, no. 1, pp. 102255, 2020, https://doi.org/10.1016/j.scs.2020.102255.
[23] M. Kharrich, O. H. Mohammed, N. Alshammari, and M. Akherraz, "Multi-objective optimization and the effect of the economic factors on the design of the microgrid hybrid system," *Sustain. Cities Soc*., vol. 65, no. 1, pp. 102646, 2021, https://doi.org/10.1016/j.scs.2020.102646.
[24] H. M. Usman, M. Sulaiman, M. S. Yahaya, and S. Saminu, "Stabilizing environmental conditions for improved biogas generation: A comparative analysis of above-ground and underground plastic digester in fed-batch systems," *Iranica J. Energy & Environ*., vol. 16, no. 2, pp. 227–239, 2025, https://doi.org/10.5829/ijee.2025.16.02.06.
[25] F. Conteh, H. Takahashi, A. M. Hemeida, N. Krishnan, A. Mikhaylov, and T. Senjyu, "Analysis of hybrid grid-connected renewable power generation for sustainable electricity supply in Sierra Leone," *Sustainability*, vol. 13, no. 20, pp. 11435, 2021, https://doi.org/10.3390/su132011435.

[26] H. M. Usman, M. S. Yahaya, S. Saminu, M. Muhammad, S. Ibrahim, B. I. Sani, and M. Sulaiman, "Design modification and performance evaluation of solar PV system at AutoCAD laboratory," *in Leveraging Artificial Intelligence to Achieve United Nations Sustainable Development Goals*, Jun. 2024, https://hal.science/hal-04654019/.
[27] T. Ma, H. Yang, and L. Lu, "A feasibility study of a stand-alone hybrid solar–wind–battery system for a remote island," *Appl. Energy*, vol. 121, no. 15, pp. 149–158, 2014, https://doi.org/10.1016/j.apenergy.2014.01.090.
[28] H. M. Usman, M. Mahmud, M. S. Yahaya, and S. Saminu, "Wind-powered agriculture: Enhancing crop production and economic prosperity in arid regions," *Elektrika*, vol. 16, no. 1, pp. 10–19, 2024, https://doi.org/10.26623/elektrika.v16i1.8999.
[29] S. K. Nandi and H. R. Ghosh, "A wind–PV-battery hybrid power system at Sitakunda in Bangladesh," E*nergy Policy*, vol. 37, no. 9, pp. 3659–3664, 2009, https://doi.org/10.1016/j.enpol.2009.04.039.
[30] A. Al-Sharafi, A. Z. Sahin, T. Ayar, and B. S. Yilbas, "Techno-economic analysis and optimization of solar and wind energy systems for power generation and hydrogen production in Saudi Arabia," *Renew. Sustain. Energy Rev*., vol. 69, no. 1, pp. 33–49, 2017, https://doi.org/10.1016/j.rser.2016.11.157.
[31] B. A. Nouadje, P. T. Kapen, V. Chegnimonhan, and R. Tchinda, "Techno-economic analysis of an islanded energy system based on geothermal/biogas/wind/PV utilizing battery technologies: A case study of Woulde, Adamawa's region, Cameroon," *Energ. Strat. Rev*., vol. 54, no. 1, pp. 101469, 2024, https://doi.org/10.1016/j.esr.2024.101469.
[32] G. F. Tajouo, P. T. Kapen, and F. L. Koffi, "Techno-economic investigation of an environmentally friendly small-scale solar tracker-based PV/wind/Battery hybrid system for off-grid rural electrification in the Mount Bamboutos, Cameroon," *Energ. Strat. Rev.*, vol. 48, no. 1, pp. 101107, 2023, https://doi.org/10.1016/j.esr.2023.101107.
[33] H. M. Usman, N. K. Sharma, D. K. Joshi, A. Kaushik, and S. Saminu, "Innovative optimization of microgrid configuration for sustainable, reliable, and economical energy using HOMER software," 2024, https://doi.org/10.21203/rs.3.rs-4520716/v1.
[34] P. T. Kapen, B. A. Nouadje, V. Chegnimonhan, G. Tchuen, and R. Tchinda, "Techno-economic feasibility of a PV/battery/fuel cell/electrolyzer/biogas hybrid system for energy and hydrogen production in the far north region of Cameroon by using HOMER Pro," *Energ. Strat. Rev*., vol. 44, no. 1, pp. 100988, 2022, https://doi.org/10.1016/j.esr.2022.100988.
[35] H. M. Usman, N. K. Sharma, D. K. Joshi, B. I. Sani, M. Mahmud, S. Saminu, and R. S. Auwal, "Optimization of grid-connected PV systems: Balancing economics and environmental sustainability in Nigeria," *Buletin Ilmiah Sarjana Teknik Elektro*, vol. 6, no. 3, pp. 237–253, 2024, https://doi.org/10.21203/rs.3.rs-4886066/v1.
[36] T. O. Araoye, E. C. Ashigwuike, M. J. Mbunwe, O. I. Bakinson, and T. I. Ozue, "Techno-Economic Modeling and Optimal Sizing of Autonomous Hybrid Microgrid Renewable Energy System for Rural Electrification Sustainability using HOMER and Grasshopper Optimization Algorithm," *Renewable Energy*, vol. 120712, 2024, https://doi.org/10.1016/j.renene.2024.120712.
[37] C. G. Lewis, M. W. Ijeoma, R. O. Yakubu, B. N. Chukwu, H. Chen, and M. Carbajales-Dale, "Achieving universal energy access in remote locations using HOMER energy model: a techno-economic and environmental analysis of hybrid microgrid systems for rural electrification in northeast Nigeria," *Frontiers in Energy Research*, vol. 12, p. 1454281, 2024, https://doi.org/10.3389/fenrg.2024.1454281.
[38] H. M. Falih, H. Demirel, and H. Al-Bayaty, "Determining the optimal parameters of a hybrid microgrid for supplying the University of Kirkuk in Iraq," *in 2024 12th International Conference on Smart Grid (icSmartGrid)*, pp. 693-698, May 2024, https://doi.org/10.1109/icSmartGrid61824.2024.10578148.
[39] P. Netshilonwe, F. Nemangwele, and M. Ratshitanga, "An Economic Performance Overview of Microgrids for Limpopo Province Rural Areas," *in 2024 IEEE PES/IAS PowerAfrica*, pp. 1-7, 2024, https://doi.org/10.21203/rs.3.rs-4520716/v1.
[40] M. F. Ali, M. A. Hossain, M. M. Julhash, M. Ashikuzzaman, M. S. Alam, and M. R. I. Sheikh, "A Techno-Economic Analysis of a Hybrid Microgrid System in a Residential Area of Bangladesh: Optimizing Renewable Energy," *Sustainability (2071-1050)*, vol. 16, no. 18, 2024, https://doi.org/10.3390/su16188051.
[41] P. K. Sahu, S. Jena, and U. Sahoo, "Techno-economic analysis of hybrid renewable energy system with energy storage for rural electrification," *Hybrid Renew. Energy Syst*., vol. 12, pp. 63–96, Feb. 2021, https://doi.org/10.1002/9781119555667.ch3.
[42] T. Adefarati and G. D. Obikoya, "Techno-economic evaluation of a grid-connected microgrid system," *Int. J. Green Energy*, vol. 16, no. 15, pp. 1497–1517, Dec. 2019, https://doi.org/10.1080/15435075.2019.1671421.
[43] N. C. Alluraiah and P. Vijayapriya, "Optimization, design, and feasibility analysis of a grid-integrated hybrid AC/DC microgrid system for rural electrification," *IEEE Access*, 2023.https://doi.org/10.1109/ACCESS.2023.3291010.
[44] O. Krishan and S. Suhag, "Techno-economic analysis of a hybrid renewable energy system for an energy-poor rural community," *J. Energy Storage*, vol. 23, pp. 305–319, Jun. 2019, https://doi.org/10.1016/j.est.2019.04.002.
[45] H. Taghavifar and Z. S. Zomorodian, "Techno-economic viability of on grid micro-hybrid PV/wind/Gen system for an educational building in Iran," *Renew. Sustain. Energy Rev*., vol. 143, Art. no. 110877, Jun. 2021, https://doi.org/10.1016/j.rser.2021.110877.
[46] H. K. Pujari and M. Rudramoorthy, "Optimal design, prefeasibility techno-economic and sensitivity analysis of off-grid hybrid renewable energy system," *Int. J. Sustain. Energy*, vol. 12, no. 1, pp. 1–33, 2022, https://doi.org/10.1080/14786451.2022.2058502.
[47] G. Tay *et al.,* "Optimal sizing and techno-economic analysis of a hybrid solar PV/wind/diesel generator system," *in IOP Conference Series: Earth and Environmental Science*, vol. 1042, no. 1, p. 012014, Jul. 2022, https://doi.org/10.1088/1755-1315/1042/1/012014.

[48] A. S. Aziz, M. F. N. Tajuddin, M. R. Adzman, M. F. Mohammed, and M. A. M. Ramli, "Feasibility analysis of grid-connected and islanded operation of a solar PV microgrid system: A case study of Iraq," *Energy*, vol. 191, Art. no. 116591, Jan. 2020, https://doi.org/10.1016/j.energy.2019.116591.
[49] S. Singh, P. Chauhan, and N. Singh, "Capacity optimization of grid connected solar/fuel cell energy system using hybrid ABC-PSO algorithm," *Int. J. Hydrogen Energy*, vol. 45, no. 16, pp. 10070–10088, Mar. 2020, https://doi.org/10.1016/j.ijhydene.2020.02.018.
[50] C. A. Nallolla, "Optimal design of a hybrid off-grid renewable energy system using techno-economic and sensitivity analysis for a rural remote location," *Sustainability*, vol. 14, no. 22, p. 15393, Nov. 2022, https://doi.org/10.3390/su142215393.

BIOGRAPHY OF AUTHORS

Habib Muhammad Usman, is a Nigerian scholar specializing in renewable energy systems. He earned a first-class degree in Electrical Engineering from Ahmadu Bello University, Zaria, and has completed an MTech in Electrical Engineering (Renewable Energy) at Mewar University, India. Habib's research focuses on optimizing hybrid microgrid configurations using renewable energy sources. He has published several peer-reviewed papers on energy optimization and system, renewable energy system, electric vehicles and power electronics. Habib is an active participant in workshops and training, Habib completed programs on GAMS and Smart Grid technologies. He has also excelled in demonstrating strong teaching and mentorship skills. With a commitment to sustainability, Habib combines research, practical expertise, and academic leadership to advance renewable energy solutions globally. Email: Habibusman015@gmail.com. ORCID: https://orcid.org/0009-0004-9584-7833 .